Effects of Exponential Viscosity and Internal Heat Generation on Free Convection of Non-Newtonian Fluids Flow over A Vertical Plate in Porous Media: VWT/VWC

指數變化之黏度與內部熱源效應對於飽和多孔性介質內非牛頓流體流經一垂直

平板自然對流的影響:可變壁溫度/可變壁濃度

Kuo-Ann Yih, Uon-Jien Payne 易國安、潘永堅

Department of Aircraft Engineering, Air Force Institute of Technology 飛機工程系,空軍航空技術學院

Abstract

The effects of the exponential decaying viscosity and internal heat generation on free convection of a non-Newtonian fluid flow over a vertical flat plate embedded in a saturated-porous medium are numerically analyzed. The surface of the vertical flat plate is maintained at variable wall temperature and variable wall concentration (VWT/VWC). To obtain the similarity solution, the internal heat generation is of an exponential decaying form. The viscosity of the fluid is assumed to follow Reynolds viscosity model. The similar governing equations are obtained by using a suitable coordinate transformation and then solved by Keller box method (KBM). Comparisons with previously published work are performed and excellent agreement is obtained. Numerical data for the dimensionless temperature profile, the dimensionless concentration profile, the local Nusselt number and the local Sherwood number are presented for the viscosity parameter Ω , the internal heat generation coefficient A^* , the power-law index of the non-Newtonian fluid n, the exponent of VWT/VWC λ , the buoyancy ratio N, and the Lewis number Le. The local Nusselt number decreases as the internal heat generation coefficient A* and the Lewis number Le are increased. However, the local Sherwood number increases with A^* and Le. An increase in the power-law index n tends to retard the flow and thus reduces the local Nusselt number and the local Sherwood number. Increasing the viscosity parameter Ω , the exponent of VWT/VWC λ and the buoyancy ratio N leads to an increase in the buoyancy force, and thus increases the local Nusselt number and the local Sherwood number.

Keywords: Exponential viscosity, internal heat generation, free convection, non-Newtonian fluid, vertical flat plate, porous media

摘要

本文以一數值方法分析:指數遞減黏度與內部熱源效應,對於在飽和多孔性介質內非牛頓流體流經一垂直平板之自然對流熱傳與質傳影響。垂直平板的表面維持於可變壁溫度/可變壁濃度條件。為了要得到一相似解,內部熱源形式假設為指數漸減。流體的黏度假設為依循雷諾黏度模式。首先以合適的座標轉換可得到一組相似方程式,再以凱勒盒子法來求解。數值計算結果與已發表的論文作比較,結果非常吻合。數值計算結果主要顯示:黏度參數,內部熱源係數,非牛頓流體之冪次律指標,可變壁溫度/可變壁濃度指數,浮力比,路易士數,對於無因次溫度分佈、無因次濃度分佈、局部紐塞爾數(Nusselt number)和局部希爾吾德數於無因次溫度分佈、無因次濃度分佈、局部紐塞爾數(Nusselt number)和局部希爾吾德數的部希爾吾德數數隨著內部熱源參數與路易士數之增大而增加。當增加冪次律指標時,會降低流速,進而降低局部紐塞爾數和局部希爾吾德數數。增大黏度參數,可變壁溫度/可變壁濃度指數與浮力比,則增加局部紐塞爾數和局部希爾吾德數數。

關鍵字:指數黏度,內部熱源,自然對流,非牛頓流體,垂直平板,多孔性介質

1. Introduction

Double diffusion by free convection flow in a saturated porous medium with Newtonian and non-Newtonian fluids may be found in geophysical, geothermal and industrial applications, such as extraction of geothermal energy and disposal of underground nuclear wastes. Ingham and Pop [1] presents a comprehensive account of the available information in this field.

A number of industrially important fluids, including fossil fuels which can saturate underground beds, display the behavior of non-Newtonian. The non-linear relationship between shear strain rate and shear stress of non-Newtonian fluids in porous matrix is quite different from that of Newtonian fluids in porous media. In the aspect of pure heat transfer, Chen and Chen [2], Yih [3], Wang et al. [4] investigated the cases of the vertical flat plate [2], cone [3], and axisymmetric and two-dimensional bodies [4]. In the aspect of coupled heat and mass transfer, double-diffusion from a vertical surface in a

porous region saturated with a non-Newtonian fluid was studied by Rastogi and Poulikakos [5]. Cheng [6-7] examined the natural convection heat and mass transfer of non-Newtonian power law fluids for a vertical wavy surface [6] and vertical truncated cone [7], respectively.

The effect of internal heat generation is important in several applications that include reactors safety analyses, metal waste form development for spent nuclear fuel, fire and combustion studies, and the storage of radioactive materials. Grosan and Pop [8] extended the research of Chen and Chen [2] to investigate the free convection over the vertical flat plate with a variable wall temperature and internal heat generation in a porous medium saturated with a non-Newtonian fluid. Chamkha et al. [9] studied effect of variable suction/injection on free convection along a vertical plate in a nanofluid saturated non-Darcy porous medium with internal heat generation. Yih and Huang [10-11] analyzed the effect of internal heat generation on free convection flow of non-Newtonian fluids over a vertical flat plate [10] and vertical truncated cone [11] in porous media for the case of variable wall temperature and variable wall concentration (VWT/VWC), respectively. The work of Yih and Huang [10] ([11]) is the extension of Grosan and Pop [8] (Cheng [7]). Recently, Huang [12] studied the effect of thermal radiation and internal heat generation on natural convection from a vertical flat plate in porous media considering Soret/Dufour effects. Influence of internal heat generation and thermal radiation on the MHD-free convection of non-Newtonian fluids over a vertical permeable plate in porous media with Soret/Dufour effects was investigated by Huang [13].

In all the above-mentioned studies [2-13], the viscosity of the fluid was assumed to be constant. However, it is known that the fluid physical properties may change significantly with temperature changes. To accurately predict the flow behavior, it is necessary to take into account this variation of viscosity with temperature. Bagai [14] investigated the effect of Reynolds viscosity model (the viscosity decreases exponential with temperature) on free convection over a non-isothermal axisymmetric body in a porous medium with internal heat generation. Kairi et al. [15] studied effect of viscous dissipation on natural convection in a non-Darcy porous medium saturated with non-Newtonian fluid of variable viscosity. Mahmoud [16] analyzed variable viscosity effect on free convection of a non-Newtonian power-law fluid over a vertical cone in a porous medium with variable heat flux (VHF). Mahmoud [17] examined radiation effect on free convection of a non-Newtonian fluid over a vertical cone embedded in a porous medium with heat generation. Effect of variable viscosity on free convective heat transfer over a non-isothermal body of arbitrary shape in a non-Newtonian fluid saturated porous medium with internal heat generation Bagai and Nishad [18]. Narayana et al. [19] investigated Soret and exponential viscosity effects on the natural convection from a vertical plate in a thermally medium saturated stratified porous with non-Newtonian liquid. Makinde, and Mishra [20] studied On stagnation point flow of variable viscosity nanofluids past a stretching surface with radiative heat. Khan et al. [21] presented the non-aligned MHD stagnation point flow of variable viscosity nanofluids past a stretching sheet with radiative heat. Bioconvection in rotating system immersed in nanofluid with temperature dependent viscosity and thermal conductivity was examined by Xun [22].

The objective of the present work, therefore, is to follow Reynolds viscosity model [14-22] and extend the work of Yih and Huang [10] to investigate the exponential decaying viscosity and internal heat generation effects on heat and mass transfer by the free convection flow of a non-Newtonian fluid over a vertical flat plate embedded in a saturated-porous medium. To the best of our knowledge, this problem has not been investigated before. The governing equations have been solved numerically using Keller box method (KBM). The results are obtained for various values of the parameters.

2. Analysis

In this paper, we consider the problem of the effects of the exponential decaying viscosity and internal heat generation on combined heat and mass free convection flow of non-Newtonian fluids over a vertical flat plate embedded in a fluid-saturated porous medium. Figure 1 shows the flow model and

physical coordinate system. The origin of the coordinate system is placed at the leading edge of the vertical flat plate, where x and y are Cartesian coordinates measuring distance along and normal to the surface of vertical flat plate, respectively.

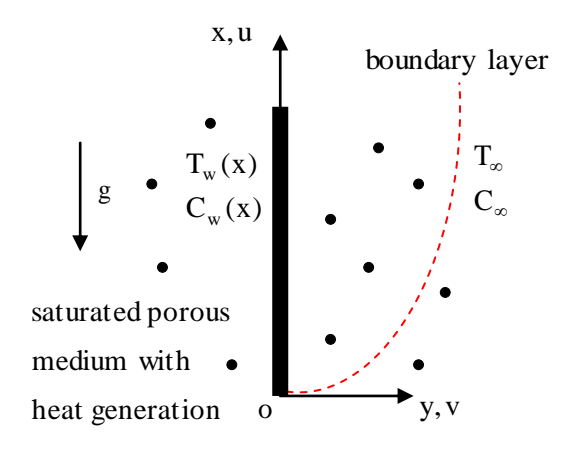


Fig. 1 Flow model and physical coordinate system

We consider the boundary condition of variable wall temperature $T_w(x)$ and variable wall concentration $C_w(x)$ (VWT/VWC); $T_w(x)$ and $C_w(x)$ are higher than the ambient temperature T_∞ and ambient concentration C_∞ , respectively. The variations of fluid properties are limited to density variation that affects the buoyancy force term only. The viscous dissipation effect is neglected for the low velocity.

Introducing the boundary layer approximation $(\partial/\partial x \ll \partial/\partial y, v \ll u)$ and Boussinesq approximation, the governing equations and the boundary conditions based on the Darcy law (It is valid under the condition of low velocity and small pores of porous medium [23]) can be written as follows [10, 14-22]:

Continuity equation:

$$\frac{\partial u}{\partial x} + \frac{\partial v}{\partial y} = 0,\tag{1}$$

Momentum (Darcy) equation:

$$\frac{\partial}{\partial y}(\mu u^n) = \rho_{\infty} g K(n) \left(\beta_T \frac{\partial T}{\partial y} + \beta_C \frac{\partial C}{\partial y} \right), \quad (2)$$

Energy equation:

$$u\frac{\partial T}{\partial x} + v\frac{\partial T}{\partial y} = \alpha \frac{\partial^2 T}{\partial y^2} + \frac{q'''}{\rho_{\infty} C_n},$$
 (3)

Concentration equation:

$$u\frac{\partial C}{\partial x} + v\frac{\partial C}{\partial y} = D_M \frac{\partial^2 C}{\partial y^2},\tag{4}$$

Boussinesq approximation:

$$\rho = \rho_{\infty} \left[1 - \beta_T \left(T - T_{\infty} \right) - \beta_C \left(C - C_{\infty} \right) \right], \quad (5)$$

Boundary conditions:

y=0:
$$v=0$$
, $T = T_w(x) = T_{\infty} + a_1 x^{\lambda}$,
 $C = C_w(x) = C_{\infty} + b_1 x^{\lambda}$, (6)

$$y \to \infty$$
: $u = 0$, $T = T_{\infty}$, $C = C_{\infty}$. (7)

Here, u and v are the Darcian velocities in the x- and y- directions; K(n) is the modified permeability of the porous medium; g is the gravitational acceleration; μ , p and ρ are the modified viscosity, the pressure and the density of the fluid, respectively; T and C are the volume-averaged temperature and concentration, respectively; α and D_M are the equivalent thermal diffusivity and mass diffusivity, respectively; q''' is the internal heat generation rate per unit volume; C_p is the specific heat at constant pressure; β_T and β_C are the thermal and concentration expansion coefficients of the fluid, respectively; α_I and α_I are positive constants; α_I is the exponent of VWT/VWC.

The fluid is Newtonian at the power-law index n = 1; n < 1 and n > 1 correspond to pseudo-plastic and dilatant fluids, respectively. The power law model of Ostwald-de-Waele adopted is according to Christopher and Middleman [24] and Dharmadhikari and Kale [25].

The stream function ψ is defined by

$$u = \partial \psi / \partial y$$
, $v = -\partial \psi / \partial x$. (8)

Therefore, the continuity equation is automatically satisfied.

Integrating equation (2) once and with the aid of equation (7), then we get

$$\mu u^n = \rho_\infty g K(n) \left[\beta_T (T - T_\infty) + \beta_C (C - C_\infty) \right]$$
 (9)

Invoking the following dimensionless similarity variables:

$$\eta = \frac{y}{x} R a_x^{1/2n} \tag{10.1}$$

$$f(\eta) = \frac{\psi}{\alpha R a_{x}^{\frac{1}{2}n}}$$
 (10.2)

$$\theta(\eta) = \frac{T - T_{\infty}}{T_{w}(x) - T_{\infty}} \tag{10.3}$$

$$\phi(\eta) = \frac{C - C_{\infty}}{C_{w}(x) - C_{\infty}}$$
 (10.4)

$$Ra_{x} = \frac{\rho_{\infty}g\beta_{T}\left[T_{w}(x) - T_{\infty}\right]K(n)}{\mu_{\infty}\left(\frac{x}{\alpha}\right)^{n}} (10.5)$$

where Ra_x is the local Rayleigh number for the flow through the porous medium.

The internal heat generation rate per unit volume q''' is modeled according to the following equation [8-13]:

$$q''' = A^* \frac{k R a_x^{\gamma_n}}{x^2} [T_w(x) - T_\infty] e^{-\eta}.$$
 (11)

Here, k is the equivalent thermal conductivity. A^* is the coefficient of internal heat generation. Note that when $A^* = 0$, this case corresponds to the absence of internal heat generation while for $A^* > 0$, the case corresponds to the presence of internal heat generation.

The fluid viscosity obeying Reynolds viscosity model is given by [14-22]:

$$\mu(\theta) = \mu_{\infty} e^{-\Omega \theta}. \tag{12}$$

where μ_{∞} is the viscosity at the ambient medium and Ω is the dimensionless viscosity parameter depending

on the nature of the fluid. This model can be applicable in many processes where pre-heating of the fuel is used as a means to enhanced heat transfer effect. Besides, for many fluids such as lubricants, polymers, an appropriate constitutive relation where viscosity is a function of temperature should be used [15].

Substituting equations (10)-(12) into equations (9), (3)-(4), (6)-(7), we can obtain

$$e^{-\Omega\theta} (f')^n = \theta + N \phi, \tag{13}$$

$$\theta'' + \frac{n+\lambda}{2n} f \theta' - \lambda f'\theta + A^* e^{-\eta} = 0, \quad (14)$$

$$\frac{1}{Le}\phi'' + \frac{n+\lambda}{2n}f\phi' - \lambda f'\phi = 0. \tag{15}$$

The boundary conditions are defined as follows:

$$\eta = 0: f = 0, \theta = 1, \phi = 1,$$
(16)

$$\eta \to \infty$$
: $\theta = 0, \ \phi = 0.$ (17)

where primes denote differentiation with respect to η . Besides, the buoyancy ratio N and the Lewis number Le are defined as follows, respectively:

$$N = \frac{\beta_C \left[C_w(x) - C_\infty \right]}{\beta_T \left[T_w(x) - T_\infty \right]} = \frac{\beta_C b}{\beta_T a}, \quad Le = \frac{\alpha}{D_M}. \quad (18)$$

In addition, in terms of the new variables, the Darcian velocities in *x*- and *y*- directions are, respectively, given by

$$u = \frac{\alpha R a_x^{\gamma_n}}{r} f', \tag{19}$$

$$v = -\frac{\alpha R a_x^{\frac{1}{2}n}}{x} \left[\left(\frac{n+\lambda}{2n} \right) f - \left(\frac{n-\lambda}{2n} \right) \eta f' \right].$$
 (20)

The results of practical interest in many applications are both the surface heat and mass transfer rates. The surface heat and mass transfer rates are expressed in terms of the local Nusselt number Nu_x and the local Sherwood number Sh_x respectively, which are basically defined as follows:

$$Nu_x = \frac{h_x x}{k} = \frac{q_w x}{[T_w(x) - T_\infty] k}.$$
 (21)

$$Sh_{x} = \frac{h_{m,x}x}{D_{M}} = \frac{m_{w}x}{\left[C_{w}(x) - C_{\infty}\right]D_{M}}.$$
 (22)

where h_x , $h_{m,x}$ are local convective heat transfer coefficient and local convective mass transfer coefficient, respectively; q_w and m_w are the local heat flux and the local mass flux, respectively; and $q_w = h_x \big[T_w(x) - T_\infty \big]$ (the Newton's law of cooling) and $m_w = h_{m,x} \big[C_w(x) - C_\infty \big]$ (the analogy between the mass transfer and the heat transfer).

From the Fourier's law of heat conduction and the Fick's law of mass diffusion, the rate of surface heat transfer q_w and the rate of surface mass transfer m_w are defined as follows, respectively:

$$q_w = -k \left(\frac{\partial T}{\partial y} \right) \Big|_{y=0}, \quad m_w = -D_M \left(\frac{\partial C}{\partial y} \right) \Big|_{y=0}.$$
 (23)

Inserting equation (23) into equations (21)-(22) and with the aid of equation (10), the local Nusselt number Nu_x and the local Sherwood number Sh_x in terms of $Ra_x^{\frac{1}{2}n}$ are, respectively, obtained by

$$\frac{Nu_x}{Ra_x^{\frac{1}{2}n}} = [-\theta'(0)], \qquad \frac{Sh_x}{Ra_x^{\frac{1}{2}n}} = [-\phi'(0)]. \quad (24)$$

For the case of $\Omega = 0$, equations (13)-(17), are reduced to those of Yih and Huang [10] where a similar solution was obtained previously.

3. Numerical Method

The present analysis integrates the system of equations (13)-(17) by the implicit finite difference approximation together with the modified Keller box method of Cebeci and Bradshaw [26]. The Keller box method comprises four stages: 1) Decomposition of the N^{th} order partial differential equation system to N^{th} first order equations. 2) Finite difference

discretization. 3) Quasi-linearization of non-linear Keller algebraic equations. 4) Block-tridiagonal elimination solution of the linearized Keller algebraic equations. To begin with, the differential equations are first converted into a system of five first-order equations. Then these first-order equations are expressed in finite difference forms and solved along with their boundary conditions by an iterative scheme. This approach gives a better rate of convergence and reduces the numerical computational times.

Computations were carried out on a personal computer with the first step size $\Delta \eta_1 = 0.01$. The variable grid parameter is chosen 1.01 and the value of $\eta_{\infty} = 20$. The iterative procedure is stopped to give the final temperature and concentration distributions when the errors in computing the θ'_w and ϕ'_w in the next procedure become less than 10^{-5} .

4. Results and Discussion

In order to verify the accuracy of our present method, we have compared our results with those of Yih [27], Bejan and Khair [28], Wang et al. [4], Bagai [14], Bagai and Nishad [18], Grosan and Pop [8], Yih and Huang [11].

Table 1 illustrates the comparison of values of $Nu_x/Ra_x^{1/2n}$ and $Sh_x/Ra_x^{1/2n}$ for various values of λ with N=1, Le=10, n=1, $A^*=0$, $\Omega=0$, respectively. Table 2 shows the comparison of values of $Nu_x/Ra_x^{1/2n}$ for various values of $n=\lambda$ with $N=A^*=\Omega=0$. Table 3 displays the comparison of values of $Nu_x/Ra_x^{1/2n}$ for various values of λ and λ with λ 0 with λ 1 and λ 2 with λ 2 and λ 3 with λ 4 and λ 5 with λ 5 and λ 6 with λ 6 with λ 8 and λ 9 with λ 9 w

 $Sh_x/Ra_x^{\frac{1}{2}n}$ for various values of n, λ and A^* with N=4, Le=10, $\Omega=0$, respectively.

The comparisons in all the above cases are found to be in excellent agreement, as shown in Tables 1-6. The value of the heat transfer is negative in Tables 3-5. It means the heat transfer from the porous medium to the plate.

Table 1 Comparison of values of $Nu_x/Ra_x^{\frac{1}{2}n}$ and $Sh_x/Ra_x^{\frac{1}{2}n}$ for various values of λ with $N=1, Le=10, n=1, A^*=0, \Omega=0$

	Nu _x	$/Ra_x^{\frac{1}{2}n}$	$Sh_x/Ra_x^{1/2n}$	
λ	Yih [27]	Present results	Yih [27]	Present results
0.0	0.5215	0.5214 (0.521)	2.2021	2.2019 (2.202)
1/3	0.8053	0.8053	3.3394	3.3390
1/2	0.9179	0.9179	3.7900	3.7895
1.0	1.1967	1.1967	4.9064	4.9055

Results in parentheses are those of Bejan and Khair [28]

Table 2 Comparison of values of $Nu_x/Ra_x^{\frac{1}{2n}}$ for various values of $n = \lambda$ with $N = A^* = \Omega = 0$

$n = \lambda$	$Nu_x / Ra_x^{\frac{1}{2}n}$			
	Wang et al. [4]	Present results		
0.25	0.5000	0.5000		
0.5	0.7071	0.7071		
0.75	0.8660	0.8660		
1	1.0000	1.0000		
1.5	1.2247	1.2247		
2.0	1.4142	1.4142		
3.0	1.7321	1.7320		

Table 3 Comparison of values of $Nu_x/Ra_x^{\frac{1}{2}n}$ for various values of λ and Ω

with
$$n = A^* = 1$$
, $N = 0$

	$Nu_x / Ra_x^{\frac{1}{2}n}$					
λ	$\Omega = 0.1$		$\Omega = 0.5$			
	Bagai [14]	Present results	Bagai [14]	Present results		
0.0	-0.1900	-0.1892	-0.0800	-0.0792		
0.5	0.2751	0.2750	0.4411	0.4412		
1.0	0.5716	0.5713	0.7748	0.7746		

Table 4 Comparison of values of $Nu_x / Ra_x^{\frac{1}{2}n}$ for various values of n, λ and Ω

with
$$A^* = 1, N = 0$$

		$Nu_x/Ra_x^{\gamma_{2n}}$				
		$\Omega = 0.0$		$\Omega = 0.75$		
n	λ	Bagai and Nishad [18]	Present results	Bagai and Nishad [18]	Present results	
0.5	0.0	-0.2574	-0.2576	0.1659	0.1658	
	1/3	(0.0800)	0.0802	_	0.7006	
	1.0	(0.4697)	0.4698	_	1.3382	
1	0.0	-0.2152	-0.2153	-0.0053	-0.0054	
	1/3	(0.1141)	0.1141		0.4003	
	1.0	(0.5254)	0.5241	_	0.9151	
2.0	0.0	-0.1780	-0.1780	-0.0725	-0.0725	
	1/3	(0.1457)	0.1457	_	0.2869	
	1.0	(0.5699)	0.5686	_	0.7563	

Results in parentheses are those of Grosan and Pop [8]

Table 5 Comparison of values of $Nu_x / Ra_x^{\frac{1}{2}n}$ for

various values of n, λ and A^* with N = 4, Le = 10, $\Omega = 0$

	λ	$Nu_x / Ra_x^{\frac{1}{2}n}$			
n		$A^* = 0$		$A^* = 1$	
		Yih and Huang [11]	Present results	Yih and Huang [11]	Present results
0.5	0.0	1.0105	1.0104	0.2404	0.2402
	0.5	1.9584	1.9584	1.2846	1.2846
1	0.0	0.6811	0.6810	-0.0191	-0.0192
	0.5	1.2206	1.2206	0.6468	0.6468
2.0	0.0	0.6030	0.6030	-0.0837	-0.0837
	0.5	1.0203	1.0203	0.4604	0.4604

Table 6 Comparison of values of $Sh_x/Ra_x^{\frac{1}{2}n}$ for various values of n, λ and A^*

with
$$N = 4$$
, $Le = 10$, $\Omega = 0$

	λ	$Sh_x/Ra_x^{\frac{1}{2}n}$			
n		$A^* = 0$		$A^* = 1$	
,,		Yih and Huang [11]	Present results	Yih and Huang [11]	Present results
0.5	0.0	6.3671	6.3671	6.4412	6.4413
	0.5	11.9022	11.9022	11.9786	11.9786
1	0.0	3.2892	3.2892	3.3311	3.3311
	0.5	5.6856	5.6856	5.7266	5.7266
2.0	0.0	2.4022	2.4022	2.4247	2.4247
	0.5	3.9682	3.9682	3.9901	3.9901

The following numerical results are graphically and tabularly presented for the buoyancy ratio N=1, the Lewis number Le=10, the viscosity parameter Ω ranging from 0 (constant viscosity) to 1, the internal heat generation coefficient $A^*=0$ (without internal

heat generation) and 1, the power-law index of the non-Newtonian fluid n=0.5 (pseudo-plastic fluid) and 2.0 (dilatant fluid), and the exponent of VWT/VWC $\lambda=0$ (uniform wall temperature and uniform wall concentration) and 1.

The effects of the viscosity parameter Ω and the internal heat generation coefficient A^* on the dimensionless temperature and concentration profiles for N = 1, Le = 10, $\lambda = 0$, n = 2.0, are shown in Figs. 2 and 3, respectively. In Fig. 2, on the one hand, for the fixed Ω , it is observed that the dimensionless temperature profile $\theta(\eta)$ increases with increasing the internal heat generation coefficient A*, thus thickening the thermal boundary layer thickness, i.e., δ_T , yet decreasing the dimensionless wall temperature gradient, i.e., $[-\theta'(0)]$. Besides, there is an overshoot in the dimensionless temperature profile for the case of $\Omega = 0$, $A^* = 1$ where heat transfer is from the porous medium to the vertical flat plate. The phenomenon of overshoot is also found in work of Yih and Huang [11-12].

On the other hand, for the fixed A^* , increasing the viscosity parameter Ω enhances the dimensionless wall temperature gradient. With the aid of equation (12), increasing the viscosity parameter Ω tends to reduce the fluid viscosity thereby enhancing both the flow velocity and the dimensionless wall temperature gradient, yet reducing the dimensionless temperature profile and the thermal boundary layer thickness.

Fig. 3 shows that for the fixed Ω , the dimensionless concentration profile $\phi(\eta)$ decreases with increasing the internal heat generation coefficient A^* , thus thinning the concentration boundary layer thickness, i.e., δ_C . For the fixed A^* , when the viscosity parameter Ω is increased has a tendency to enhance the dimensionless wall

concentration gradient, i.e., $[-\phi'(0)]$.

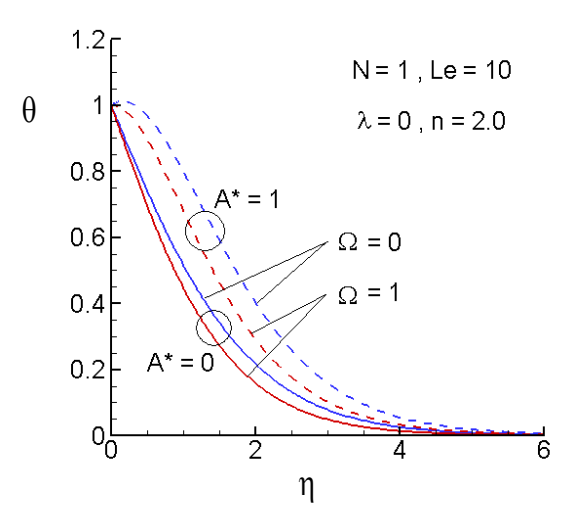


Fig. 2 Effects of the viscosity parameter and the internal heat generation coefficient on the dimensionless temperature profile

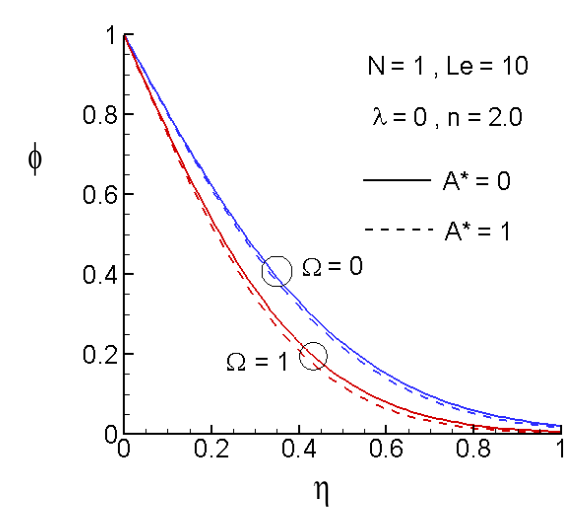


Fig. 3 Effects of the viscosity parameter and the internal heat generation coefficient on the dimensionless concentration profile

For the sake of future comparison, Tables 7 and 8 exhibit the values of $Nu_x/Ra_x^{\frac{1}{2}n}$ and $Sh_x/Ra_x^{\frac{1}{2}n}$ for various values of λ , Ω , n and A^* with N=1, Le=10, respectively. In Table 7, on the one hand, for the fixed λ , Ω and n, the local Nusselt number tends to

decrease as the internal heat generation coefficient A^* is increased. This is because increasing the internal heat generation coefficient A^* increases the thermal boundary layer thickness, as revealed in Fig. 2. The thicker the thermal boundary layer thickness, the smaller the local Nusselt number. The negative values of the local Nusselt number in Table 7 mean the heat transfer from the porous medium to the vertical flat plate.

On the other hand, for the fixed λ , n and A^* , the local Nusselt number increases as the viscosity parameter Ω is increased. This is due to the fact that increasing the viscosity parameter Ω tends to increase the dimensionless wall temperature gradient, as shown in Fig. 2. With the help of equation (24), the greater the dimensionless wall temperature gradient, the larger the local Nusselt number.

Table 7 Values of $Nu_x/Ra_x^{\frac{1}{2}n}$ for various values of λ , Ω , n and A^* with N=1, Le=10

		$Nu_x / Ra_x^{1/2n}$			
λ	Ω	n =	= 0.5	n = 2.0	
		$A^* = 0$	$A^* = 1$	$A^* = 0$	$A^* = 1$
0	0.0	0.5395	-0.1324	0.5328	-0.1451
	1/4	0.6641	0.0240	0.5566	-0.1092
	1/2	0.8199	0.2052	0.5818	-0.0723
	3/4	1.0151	0.4194	0.6083	-0.0343
	1.0	1.2599	0.6769	0.6362	0.0048
1	0.0	1.3633	0.8555	1.1497	0.6601
	1/4	1.6784	1.1976	1.2022	0.7253
	1/2	2.0723	1.6115	1.2574	0.7930
	3/4	2.5651	2.1177	1.3157	0.8633
	1.0	3.1824	2.7422	1.3771	0.9364

In Table 8, for the fixed λ , n and Ω , the local Sherwood number tends to increase slightly as the internal heat generation coefficient A^* is increased. This is due to the fact that increasing the internal heat generation coefficient A^* decreases slightly the concentration boundary layer thickness, as unveiled in Fig. 3. The thinner the concentration boundary layer thickness, the greater the local Sherwood number.

For the fixed λ , n and A^* , the local Sherwood number increases as the viscosity parameter Ω is increased. This is owing to the fact that enhancing the viscosity parameter Ω increases the dimensionless wall concentration gradient, as shown in Fig. 3. With the aid of equation (24), the greater the dimensionless wall concentration gradient, the larger the local Sherwood number.

Table 8 Values of $Sh_x/Ra_x^{\frac{1}{2}n}$ for various values of λ , Ω , n and A^* with N=1, Le=10

		$Sh_{x}/Ra_{x}^{\frac{1}{2}n}$			
λ	Ω	n =	0.5	n = 2.0	
		$A^* = 0$	$A^* = 1$	$A^* = 0$	$A^*=1$
0	0.0	2.8019	2.9426	1.9713	2.0115
	1/4	3.5483	3.7350	2.0855	2.1384
	1/2	4.4971	4.7283	2.2066	2.2721
	3/4	5.7031	5.9782	2.3352	2.4130
	1.0	7.2358	7.5555	2.4716	2.5616
1	0.0	6.8367	6.9721	4.1713	4.2092
	1/4	8.6511	8.8261	4.4113	4.4599
	1/2	10.9542	11.1683	4.6659	4.7249
	3/4	13.8752	14.1293	4.9360	5.0051
	1.0	17.5734	17.8702	5.2227	5.3014

Moreover, decreasing the power-law index n tends to increase the velocity of the flow, thereby enhancing the local Nusselt number and the local Sherwood number. Thus, the pseudo-plastic fluids (n = 0.5) are superior to the dilatant fluids (n = 2.0) from the viewpoint of the free convection heat and mass transfer rates from a vertical plate embedded in a porous medium saturated with non-Newtonian power-law fluids. This result corresponds with the work of Cheng [7]. Increasing the exponent of VWTVWC λ tends to increase the buoyancy force, accelerating the flow and thereby increasing the local Nusselt number and the local Sherwood number. Similar behavior was observed by Yih and Huang [10-11].

5. Conclusions

A laminar boundary layer analysis is presented to study the effects of exponential decaying viscosity and internal heat generation on natural convection flow of non-Newtonian power-law fluids in a Darcy porous medium resulting from combined heat and mass buoyancy effects adjacent to the vertical flat plate maintained at variable wall temperature and variable wall concentration (VWT/VWC). The Ostwald–de Waele power-law model is used to characterize the non-Newtonian behavior of the fluid. The viscosity of the fluid is assumed to follow Reynolds viscosity model. The internal heat generation is of an exponential decaying form.

Enhancing the viscosity parameter Ω , the buoyancy ratio N and the exponent of VWT/VWC λ tends to increase the local Nusselt number as well as the local Sherwood number. The local Nusselt

(Sherwood) number tends to decrease (increase) as both the internal heat generation coefficient A^* and the Lewis number Le are increased. In addition, a decrease in the power-law index n of fluids tends to increase the heat and mass transfer.

Nomenclature

- A* internal heat generation coefficient
- a_1 positive constant
- b_1 positive constant
- C concentration
- C_p specific heat at constant pressure
- D_M mass diffusivity
- f dimensionless stream function
- g gravitational acceleration
- h_x local convective heat transfer coefficient
- $h_{m,r}$ local convective mass transfer coefficient
- K(n) modified permeability of the porous medium
- k equivalent thermal conductivity
- Le Lewis number
- m_w local wall mass flux
- N buoyancy ratio
- Nu_r local Nusselt number
- n power-law index of the non-Newtonian fluid
- p pressure
- q''' internal heat generation rate per unit volume
- q_w local wall heat flux
- Ra_x modified local Rayleigh number
- Sh_x local Sherwood number
- T temperature
- u Darcy velocity in the x-direction
- v Darcy velocity in the y-direction
- x streamwise coordinate
- y transverse coordinate

Greek symbols

 α equivalent thermal diffusivity

- β_C coefficient of concentration expansion
- β_T coefficient of thermal expansion
- δ_C concentration boundary layer thickness
- δ_T thermal boundary layer thickness
- η similarity variable
- θ dimensionless temperature
- λ exponent of VWT/VWC
- μ viscosity
- ρ density
- ϕ dimensionless concentration
- ψ stream function
- Ω viscosity parameter

Subscripts

- w condition at the wall
- ∞ ambient

References

- [1] Ingham, D., and Pop, I., Transport phenomena in porous media II. Pergamon, Oxford, 2002.
- [2] Chen, H. T., and Chen, C. K., "Free convection of non-Newtonian fluids along a vertical plate embedded in a porous medium," ASME Journal of Heat Transfer, Vol. 110, pp. 257-260 (1988).
- [3] Yih, K. A., "Uniform lateral mass flux effect on natural convection of non-Newtonian fluids over a cone in porous media," International Communications in Heat and Mass Transfer, Vol. 25, pp. 959-968 (1998).
- [4] Wang, S. C., Chen, C. H., and Yang, Y. T., "Natural convection of non-Newtonian fluids through permeable axisymmetric and two-dimensional bodies in a porous medium," International Journal of Heat and Mass Transfer, Vol. 45, pp. 393-408 (2002).
- [5] Rastogi, S. K., and Poulikakos, D., "Double-diffusion from a vertical surface in a

- porous region saturated with a non-Newtonian fluid," International Journal of Heat and Mass Transfer, Vol. 38, pp. 935-946 (1995).
- [6] Cheng, C. Y., "Double diffusion from a vertical wavy surface in a porous medium saturated with a non-Newtonian fluid," International Communications in Heat and Mass Transfer, Vol. 34, pp. 285-294 (2007).
- [7] Cheng, C. Y., "Natural convection heat and mass transfer from a vertical truncated cone in a porous medium saturated with a non-Newtonian fluid with variable wall temperature and concentration," International Communications in Heat and Mass Transfer, Vol. 36, pp. 585-589 (2009).
- [7] Grosan, T., and Pop, I., "Free convection over vertical flat plate with a variable wall temperature and internal heat generation in a porous medium saturated with a non-Newtonian fluid," Technische Mechanik, Vol. 21, pp. 313-318 (2001).
- [8] Chamkha, A. J., Rashad, A. M., Reddy, C. R., and Murthy, P. V. S. N., "Effect of suction/injection on free convection along a vertical plate in a nanofluid saturated non-Darcy porous medium with internal heat generation," Indian Journal of Pure and Applied Mathematics, Vol. 45, pp. 321-342 (2014).
- [9] Yih, K. A., and Huang, C. J., "Effect of internal heat generation on free convection heat and mass transfer of non-Newtonian fluids flow over a vertical plate in porous media: VWT/VWC," Journal of Aeronautics, Astronautics and Aviation, Vol. 47, pp. 115-122 (2015).
- [10] Yih, K. A., and Huang, C. J., "Effect of internal heat generation on free convection flow of non-Newtonian fluids over a vertical truncated

- cone in porous media: VWT/VWC," Journal of Air Force Institute of Technology, Vol. 14, pp. 1-18 (2015).
- [11] Huang, C. J., "Effect of thermal radiation and internal heat generation on natural convection from a vertical flat plate in porous media considering Soret/Dufour effects," Journal of Aeronautics, Astronautics and Aviation, Vol. 48, pp. 1-10 (2016).
- [12] Huang, C. J., "Influence of internal heat generation and thermal radiation on the MHD-free convection of non-Newtonian fluids over a vertical permeable plate in porous media with Soret/Dufour effects," JP Journal of Heat and Mass Transfer, Vol. 14, pp. 289-316 (2017).
- [13] Bagai, S., "Effect of variable viscosity on free convection over a nonisothermal axisymmetric body in a porous medium with internal heat generation," Acta Mechanica, Vol. 169, pp. 187-197 (2004).
- [14] Kairi, R. R., Murthy, P. V. S. N., and Ng, C. O., "Effect of viscous dissipation on natural convection in a non-Darcy porous medium saturated with non-Newtonian fluid of variable viscosity," The Open Transport Phenomena Journal, Vol. 3, pp. 1-8 (2011).
- [15] Mahmoud, M. A. A., "Variable viscosity effect on free convection of a non-Newtonian power-law fluid over a vertical cone in a porous medium with variable heat flux," The European Physical Journal Plus, Vol. 126, pp. 1-6 (2011).
- [16] Mahmoud, M. A. A., "Radiation effect on free convection of a non-Newtonian fluid over a vertical cone embedded in a porous medium with heat generation," Journal of Applied Mechanics and Technical Physics, Vol. 53, pp. 743-750 (2012).

- [17] Bagai, S., and Nishad, C., "Effect of variable viscosity on free convective heat transfer over a non-isothermal body of arbitrary shape in a non-Newtonian fluid saturated porous medium with internal heat generation," Transport in Porous Media, Vol. 94, pp. 277-288 (2012).
- [18] Narayana, M., Khidir, A. A., Sibanda, P., and Murthy, P. V. S. N., "Soret effect on the natural convection from a vertical plate in a thermally stratified porous medium saturated with non-Newtonian liquid," ASME Journal of Heat Transfer, Vol. 135, pp. 032501-1-10 (2013).
- [19] Makinde, O. D., and Mishra, S. R. "On stagnation point flow of variable viscosity nanofluids past a stretching surface with radiative heat," International Journal of Applied and Computational Mathematics, Vol. 107, pp. 1–18 (2015).
- [20] Khan, W. A., Makinde, O. D., and Khan, Z. H., "Non-aligned MHD stagnation point flow of variable viscosity nanofluids past a stretching sheet with radiative heat," International Journal of Heat and Mass Transfer, Vol. 96, pp. 525–534 (2016).
- [21] Xun, S., Zhao, J., Zheng, L., and Zhang, X., "Bioconvection in rotating system immersed in nanofluid with temperature dependent viscosity and thermal conductivity," International Journal of Heat and Mass Transfer, Vol. 111, pp. 1001–1006 (2017).
- [22] Hong, J. T., Yamada, Y., and Tien, C. L., "Effects of non-Darcian and non-uniform porosity on vertical plate- natural convection in porous media," ASME Journal of Heat Transfer, Vol. 109, pp. 356-362 (1987).
- [23] Christopher, R. V., and Middleman, S., "Power-law flow through a packed tube,"

- Industrial & Engineering Chemistry Fundamentals, Vol. 4, pp.424-426 (1965).
- [24] Dharmadhirkari, R. V., and Kale, D. D., "Flow of non-Newtonian fluids through porous media," Chemical Engineering Science, Vol. 40, pp. 527-529 (1985).
- [25] Cebeci, T., and Bradshaw, P., Physical and Computational Aspects of Convective Heat Transfer, Springer-Verlag, New York (1984).
- [26] Yih, K. A., "Coupled heat and mass transfer by free convection over a truncated cone in porous media: VWT/VWC or VHF/VMF," Acta Mechanica, Vol. 137, pp. 83-97 (1999).
- [27] Bejan, A., and Khair, K. R., "Heat and mass transfer by natural convection in a porous medium," International Journal of Heat and Mass Transfer, Vol. 28, pp. 909-918 (1985).

航空技術學院學報 第十七卷 (民國一○七年)